Published in final edited form as:

Science. 2018 August 03; 361(6401): 502–506. doi:10.1126/science.aar8638.

HAIRY MERISTEM with WUSCHEL confines CLAVATA3 expression to the outer apical meristem layers*

Yun Zhou[#1,2,3,*], **An Yan**[#1,4], **Han Han**[2,3], **Ting Li**[1,4], **Yuan Geng**[2,3], **Xing Liu**[1,3,5], and **Elliot M. Meyerowitz**[1,4,*]

[1]Division of Biology and Biological Engineering, California Institute of Technology, Pasadena, CA 91125

[2]Department of Botany and Plant Pathology, Purdue University, West Lafayette, IN 47907

[3]Purdue Center for Plant Biology, Purdue University, West Lafayette, IN 47907

[4]Howard Hughes Medical Institute, California Institute of Technology, Pasadena, CA 91125

[5]Department of Biochemistry, Purdue University, West Lafayette, IN 47907

[#] These authors contributed equally to this work.

Abstract

The control of the location and activity of stem cells depends on spatial regulation of gene activities in the stem cell niche. Using computational and experimental approaches, we have tested, and found support for, a hypothesis for gene interactions that specify the *Arabidopsis* apical stem cell population. The hypothesis explains how the WUSCHEL gene product, synthesized basally in the meristem, induces *CLAVATA3*-expressing stem cells in the meristem apex, but, paradoxically, not in the basal domain where *WUSCHEL* itself is expressed. The answer involves the activity of the small family of *HAIRY MERISTEM* genes, that prevent the activation of *CLAVATA3*, and which are expressed basally in the shoot meristem.

One Sentence Summary: The domain of stem cells in the Arabidopsis shoot apical meristem is founded on WUS expression but bounded by HAM expression.

Distinct cell types in multicellular organisms form specific patterns during development, and how the patterns are regulated is a critical question. In *Arabidopsis* shoot apical meristems (SAMs), stem cells reside at and near the apex while the cells specifying the stem cells are located more basally *(1).* Along the apical-basal axis, the homeodomain transcription factor

*To whom correspondence should be addressed. meyerow@caltech.edu and zhouyun@purdue.edu.

Author Contributions: Y.Z., A.Y., and E.M.M. conceived the research direction; Y.Z., H.H., T.L., Y.G. performed experiments; A.Y. performed modeling and simulation; Y.Z., X.L. and E.M.M. commented on the model; X.L. contributed reagents; Y.Z., A.Y., and X.L. analyzed and interpreted data; Y.Z. and E.M.M. supervised the project; Y.Z., A.Y., X.L., and E.M.M. wrote the manuscript; H.H., T.L., and Y.G. commented on the manuscript.

Data and materials availability: all data are available in the manuscript or the supplementary material.

Competing interests: The authors declare that they have no competing interests.

WUSCHEL (WUS) and the secreted peptide CLAVATA3 (CLV3) form a negative feedback loop mediating communication between the stem cells and the beneath rib meristem cells *(2–9)*. *CLV3* is highly expressed in the apical stem cells *(2–4)*, while *WUS* transcript is confined to the center of rib meristem *(5–6)*. WUS protein moves apically via plasmodesmata, cell-cell connections, into the stem cells *(10–12)* to activate *CLV3* expression, reportedly through direct binding to the *CLV3* promoter *(10,12)*. However, how the apical-basal patterns of *CLV3* and *WUS* mRNAs are initiated and maintained are unknown. One central question is, why is *CLV3* activated only by WUS that has transited into the apical stem cells but is not activated in the interior cells where WUS protein is at highest concentration, and where WUS is actively expressed? It has been proposed that either WUS requires an as-yet unidentified signal from the epidermis (L1) of the meristem for *CLV3* activation *(13–14)*, or that WUS can convert itself from a repressor to an activator when its concentration is low *(12)*. Here, we propose a different mechanism. We previously found that members of the HAIRY MERISTEM (HAM) family, GRAS-domain transcription factors, function as interacting partners of WUS to control the production of shoot stem cells *(15)*. The HAM proteins are involved in meristem regulation and the CLV3-WUS pathway *(15–18)* and *CLV3* is ectopically expressed in the rib meristem of a *ham* multiple mutant *(16)*. Using computational and experimental approaches, we show here that in the SAMs, WUS activates *CLV3* only in the absence of HAM, and in the initiating meristems, an apical-basal gradient of HAM defines the patterning of the *CLV3* expression domain.

Imaging of fluorescent reporters for both *HAM* and *CLV3* in the same living SAMs shows that the expression patterns of *HAM* and *CLV3* mRNAs are nearly complementary, with opposite concentration gradients along the apical-basal axis (Fig. 1; Fig. S1; Movie S1-S3). *HAM1* and *HAM2* are highly expressed in the rib meristem and peripheral zone in the corpus (Fig.1, Fig. S1), where *CLV3* expression is reduced. In contrast, *HAM1* and *HAM2* expression is not detected in the L1 and L2 layers of the central zone, where *CLV3* is highly expressed (Fig.1, Fig. S1). In addition, we previously showed that *HAM1*, *HAM2* and *WUS* are co-expressed in the same cells at the center of corpus *(15)* and HAM protein was not detected in the central zone *(15)*. These images (Fig.1, Fig. S1) and previous reports *(4, 7,10–12,15)* have revealed the distinct and overlapping expression patterns of WUS, *CLV3*, and HAM in the SAM (Fig. S2), which leads to the hypothesis that in the apical stem cells where HAM is absent, *CLV3* mRNA production is activated by WUS; at the basal part of the SAM where HAM proteins are present, the ability of WUS to activate *CLV3* mRNA production is suppressed.

To test this hypothesis, we first established a new 3D+t computational model to simulate the patterns of *CLV3* and *WUS* transcripts and the movement of CLV3 and WUS proteins during meristem development (See Methods). The model incorporated the current knowledge of the CLV-WUS feedback *(2–8,19)*, and included an activator of *WUS* transcription, the Organizing Center (OC) signal at the center of the meristem corpus, and it took the concentration gradient of HAM as an input. We modeled the movement of WUS protein as a passive diffusion-like transport, as previously reported *(13–14)*. Most importantly, we defined WUS as the activator of *CLV3* transcription when HAM is absent, but not when HAM protein is present. We represented CLV3 peptide as a repressor of *WUS* mRNA level and modeled its rapid apoplastic movement between cells *(8)*. This model was

able to reproduce the specific patterns of *WUS* transcript, WUS protein, and *CLV3* transcript in a wild type SAM, and these patterns were resistant to perturbations introduced by cell growth and divisions (Movie S4-S6, S8-S9). In addition, a simplified 1D+t cell layer model was able to predict the patterns of *WUS* and *CLV3* along the apical-basal axis (Movie S7), suggesting the apical-basal polarity of gene expression can be uncoupled from lateral cell proliferation. By contrast, if HAM was converted into an activator (either together with WUS or in addition to WUS) of *CLV3* transcription, we were not able to reproduce the wild-type *CLV3* mRNA pattern (Fig. S3A-B).

We further tested the hypothesis and validated the computational model by introducing a spatial perturbation of gene expression both *in silico* and *in vivo*. The fact that *HAM* protein is absent at the center of the meristem L1 layer (Fig. 1A-E, Fig. S1A-E) promoted us to test the impact on *CLV3* patterning of specifically expressing *HAM* in the L1 layer. Our model predicted that *CLV3* mRNA in the L1 layer would be dramatically reduced due to the absence of activation in the L1, and the peak of *CLV3* expression would shift into deeper cell layers (Fig. 2A-B). We reproduced this perturbation experimentally by generating *pATML1::HAM1m-GFP* (*L1-HAM*) transgenic plants that express a HAM1-GFP fusion protein in L1 (Fig. S4A-F, Movie S10-S11) from an epidermis-specific promoter *(20)*. We found that the activity of the *CLV3* reporter in L1 of the *L1-HAM* SAM was reduced compared either to the level in cells below L2 from the same *L1-HAM* SAM or the level in L1 in a wild type SAM (Fig. 2C-L). In addition, the SAMs of *L1-HAM* plants were substantially enlarged compared to the wild type (Fig. 2C-D; Fig. S5A-B), demonstrating the functional significance of keeping HAM levels low and *CLV3* high in the epidermis.

The model also predicted that a partial repression of *HAM (18, 21)* is sufficient to alter the *CLV3* pattern (Fig. S6A-B), which is consistent with the experimental results and quantitative analyses (Fig. S6A-F). This partial repression of *HAM* led to a substantial increase in *CLV3* mRNA levels (Fig. S6C-D), more cells expressing *CLV3* in the SAMs (Fig. S6E), and a basal shift of the *CLV3* expression peak (Fig. S6F).

A series of genetic perturbations was introduced further to dissect the roles of HAM and WUS in *CLV3* patterning along the apical-basal axis in the SAM. The model made the following predictions in parallel (Fig. 3A-D): When HAM is absent in a SAM, *CLV3* mRNA would be locally activated by WUS, with the concentration peak in the basal part of the SAM (Fig. 3A-B). When HAM is present in a SAM but the transcriptional activity of WUS is reduced, the *CLV3* mRNA would still be expressed in the apical part of the SAM, with the level significantly reduced (Fig. 3C). Furthermore, when HAM is absent and the transcriptional activity of WUS is reduced, *CLV3* would then be expressed in the basal part of the SAM at a reduced level (Fig. 3D). To test these predictions, we examined the *CLV3* mRNA in the SAMs of wild type, *ham1;2;3* triple loss-of-function mutants, *wus-7* partial loss-of-function mutants *(15, 22)*, and *wus-7;ham1;2;3* quadruple mutants (Fig. 3E-H). As assessed using *in situ* hybridization experiments, the *CLV3* expression domain in *ham1;2;3* shifted to the center of the rib meristem (Fig. 3F), as observed previously *(16)*, while *CLV3* mRNA level was reduced locally in the central zone in a *wus-7* SAM (Fig. 3G). In the *wus-7; ham1;2;3* SAM, *CLV3* mRNA expression shifted to the rib meristem, and its level was significantly reduced compared to that in *ham1;2;3* (Fig. 3H). In addition, the *wus-7;*

ham1;2;3 mutant displayed a much reduced SAM size (Fig. 3H), consistent with the previous finding that HAM and WUS work together in control of stem cell homeostasis *(15).* In addition to the partial loss of function (Fig. 3C), the computational model predicted that when WUS activity is completely lost (Fig. 3I-L), *CLV3* mRNA would be absent since this major activator of *CLV3* is absent, regardless whether HAM is present (Fig. 3K) or not (Fig. 3L). These predictions were validated through the *CLV3* mRNA *in situ* hybridization in the SAMs of wild type, *ham1;2;3*, *wus-1* null mutants (5), and *wus-1;ham1;2;3* quadruple mutants (Fig. 3M-P; Fig. S7). We found that *CLV3* mRNA was undetectable in both *wus-1* and *wus-1*;*ham1;2;3* plants, and *wus-1*;*ham1;2;3* showed a terminated meristem similar to that in *wus-1* (Fig. 3O-P). These results (Fig. 3) reveal distinct roles of HAM and WUS in determining *CLV3* mRNA pattern in an established SAM: WUS maintains overall *CLV3* level while HAM defines the apical-basal positioning of the *CLV3* expression domain.

We further examined whether the HAM-WUS-CLV3 regulatory loop defines the initiation of polarity during *de novo* meristem formation from leaf axils (Fig. 4A-P, Fig. S8-S9). Differently from the already established apical meristem, in the initiating axillary meristem (AM) (Stages S2 and S3) *(23–24)*, expression of *CLV3* is first seen in the corpus *(24).* To seek the underlying mechanism, we first examined the expression pattern of *HAM1* at early stages of AM initiation. At S2, *HAM1* is evenly expressed in the initiating meristem with no gradient from the epidermis to the interior cells (Fig. 4A). At S3, *HAM1* is also expressed throughout the initiating meristem, lacking a clear gradient (Fig. 4E). Both patterns are distinct from the *HAM1* pattern in the established SAMs (Fig. 1) *(15)*. When these *HAM1* patterns (Fig. 4A, E) were used as inputs for AM simulation (Fig. 4B, F), the model predicted that the *CLV3* domains in wild type would be confined to the basal part of the initiating meristems (Fig. 4C, G), suggesting that when a HAM concentration gradient does not exist or is very shallow, the *CLV3* mRNA pattern is predominantly determined by WUS concentration. These predictions are consistent with our experimental results (Fig. 4D, H) and previous observations *(24).* At late stages of AM initiation (Fig. 4I, M), the concentration gradient of *HAM1* from epidermis to interior cells has been established, comparable to its pattern in the SAMs (Fig. 1). Using this information as input (Fig. 4J, N), the model predicted that at these stages (Fig. 4K, O), *CLV3* would be expressed predominantly in the apical domain of the initiating AMs; this was experimentally validated (Fig. 4L, P; *24*). Thus the dynamic gradient of HAM drives the *CLV3* pattern dynamics during *de novo* formation of a new stem cell niche (Movie S12).

We then simulated the patterns of *CLV3* mRNA expression at different stages during AM initiation when HAM activity is absent (Fig. 4Q). The model predicted that *CLV3* expression domains would be confined to deep cell layers at all times (Fig. 4R, Movie S13-S15), which is consistent with the experimental result (Fig. 4S, T). The computational and experimental results together demonstrated that the lack of either a gradient or expression of HAM leads to similar *CLV3* RNA patterns, suggesting that the HAM concentration gradient in a meristem acts in specifying the apical-basal polarity of the *CLV3* mRNA pattern. Additionally, the defects in *CLV3* patterning during meristem initiation (Fig. 4S, T) could be the molecular basis of the shoot branching phenotypes of the *ham1;2;3* mutants *(16–18).*

Differently from previous models *(13–14, 25)*, this work, complemented by a recent theoretical study *(26)*, reveals a regulatory circuit involving three components—WUS, HAM and CLV3—that sustains both the initiation and the maintenance of the apical-basal polarity of distinct cell types in the plant apical stem cell niche.

Supplementary Material

Refer to Web version on PubMed Central for supplementary material.

Acknowledgments:

The authors are grateful to H. Yang for sharing the *HAM1m* DNA construct, and to A. Garda from Caltech and C. Layug from Purdue for technical support.

Funding: The work at Caltech was funded by NIH grant R01 GM104244, and by the Howard Hughes Medical Institute and the Gordon and Betty Moore Foundation (through Grant GBMF3406) to E.M.M. The work at Purdue was funded by a start-up package and support from the Purdue Center for Plant Biology to Y.Z.

References and Notes:

1. Meyerowitz EM , Cell 88, 299–308 (1997). [PubMed: 9039256]
2. Fletcher JC , Brand U , Running MP , Simon R , Meyerowitz EM , Science 283, 1911–1914 (1999) [PubMed: 10082464]
3. Brand U , Fletcher JC , Hobe M , Meyerowitz EM , Simon R , Science 289, 617–619 (2000) [PubMed: 10915624]
4. Brand U , Grunewald M , Hobe M , Simon R . Plant physiology 129, 565–575 (2002) [PubMed: 12068101]
5. Laux T , Mayer KF , Berger J , Jurgens G , Development 122, 87–96 (1996) [PubMed: 8565856]
6. Mayer KF et al., Cell 95, 805–815 (1998) [PubMed: 9865698]
7. Schoof H et al., Cell 100, 635–644 (2000). [PubMed: 10761929]
8. Nimchuk ZL , Tarr PT , Ohno C , Qu X , Meyerowitz EM , Current biology 21, 345–352 (2011) [PubMed: 21333538]
9. Nimchuk ZL , Zhou Y , Tarr PT , Peterson BA , Meyerowitz EM , Development 142, 1043–1049 (2015). [PubMed: 25758219]
10. Yadav RK et al., Genes & development 25, 2025–2030 (2011). [PubMed: 21979915]
11. Daum G , Medzihradszky A , Suzaki T , Lohmann JU , PNAS 111, 14619–14624 (2014) [PubMed: 25246576]
12. Perales M et al., PNAS 113, E6298–E6306 (2016) [PubMed: 27671653]
13. Jonsson H et al., Bioinformatics 21, 232–240 (2005)
14. Gruel J et al., Science advances 2, e1500989 (2016) [PubMed: 27152324]
15. Zhou Y et al. Nature 517(7534):377–380 (2015) [PubMed: 25363783]
16. Schulze S , Schafer BN , Parizotto EA , Voinnet O , Theres K , The Plant journal 64, 668–678 (2010). [PubMed: 21070418]
17. Engstrom EM et al. Plant physiology 155, 735–750 (2011). [PubMed: 21173022]
18. Wang L , Mai YX , Zhang YC , Luo Q , Yang HQ , Molecular plant 3, 794–806 (2010). [PubMed: 20720155]
19. Muller R , Borghi L , Kwiatkowska D , Laufs P , Simon R , The Plant cell 18, 1188–1198 (2006) [PubMed: 16603652]
20. Lu P , Porat R , Nadeau JA , O'Neill SD , The Plant cell 8, 2155– 2168 (1996) [PubMed: 8989876]
21. Llave C , Xie Z , Kasschau KD , Carrington JC , Science 297, 2053–2056 (2002). [PubMed: 12242443]
22. Graf P et al., The Plant cell 22, 716–728 (2010) [PubMed: 20228247]

23. Long J , Barton MK , Developmental biology 218, 341–354 (2000) [PubMed: 10656774]
24. Xin W , Wang Z , Liang Y , Wang Y , Hu Y , Journal of plant physiology 214,1–6 (2017) [PubMed: 28399422]
25. Chickarmane VS et al., PNAS 109, 4002– 4007 (2012) [PubMed: 22345559]
26. Gruel J , Deichmann J , Landrein B , Hitchcock T , Jönsson H , bioRxiv doi: 10.1101/237933
27. Reddy GV et al., Development 131, 4225–4237 (2004) [PubMed: 15280208]
28. Cunha A et al., Methods in cell biology 110, 285–323 (2012) [PubMed: 22482954]
29. Clough SJ , Bent AF , The Plant journal 16, 735–743 (1998) [PubMed: 10069079]
30. Roeder AH , Cunha A , Ohno CK , Meyerowitz EM , Development 139, 4416–4427 (2012) [PubMed: 23095885]
31. Li W et al., Science signaling 6, ra23cr (2013) [PubMed: 23572147]
32. Zhang X et al., The Plant cell 25, 83–101 (2013) [PubMed: 23335616]
33. Krizek BA , Developmental genetics 25, 224–236 (1999) [PubMed: 10528263]

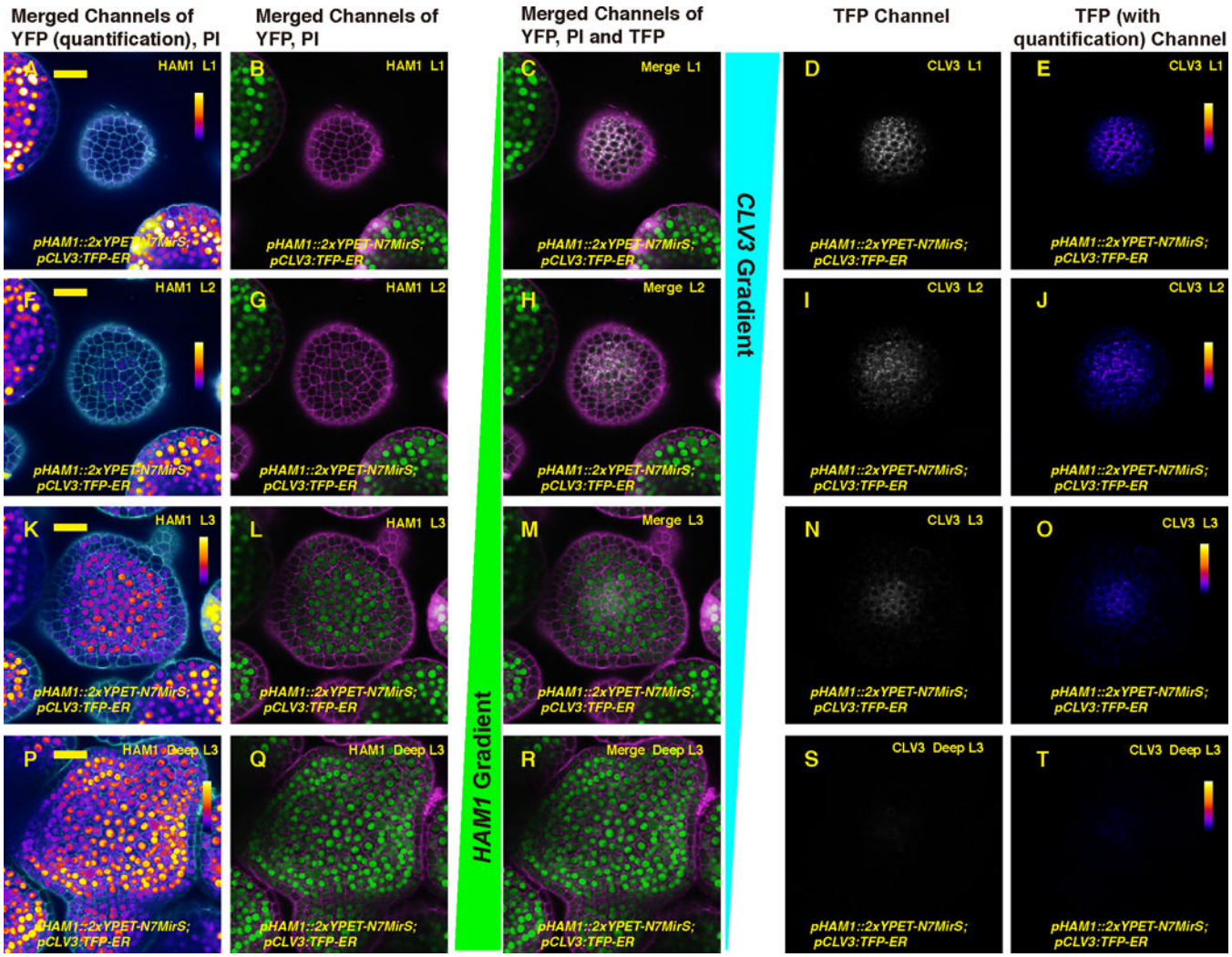

Fig. 1.

Expression patterns of *HAM1* and *CLV3* in the SAM are largely complementary. (A-T) Expression of *pHAM1::2xYPET-N7MirS* and *pCLV3::TFP-ER* in transverse optical sections from top to bottom through the same *Arabidopsis* SAM, including L1 (A-E), L2 (F-J), cells just below the L2 (K-O), and deeper layers in the center, and all layers on the meristematic periphery (P-T). Panels (from left to right): YFP (quantification indicated by color) and propidium iodide (PI) counterstain (white); YFP (green) and PI counterstain (purple); merge of three channels: YFP (green), PI (purple) and TFP (gray); TFP (gray); and TFP (quantification indicated by color). Scale bar (A-T): 20 μm; color bar: fire quantification of signal intensity.

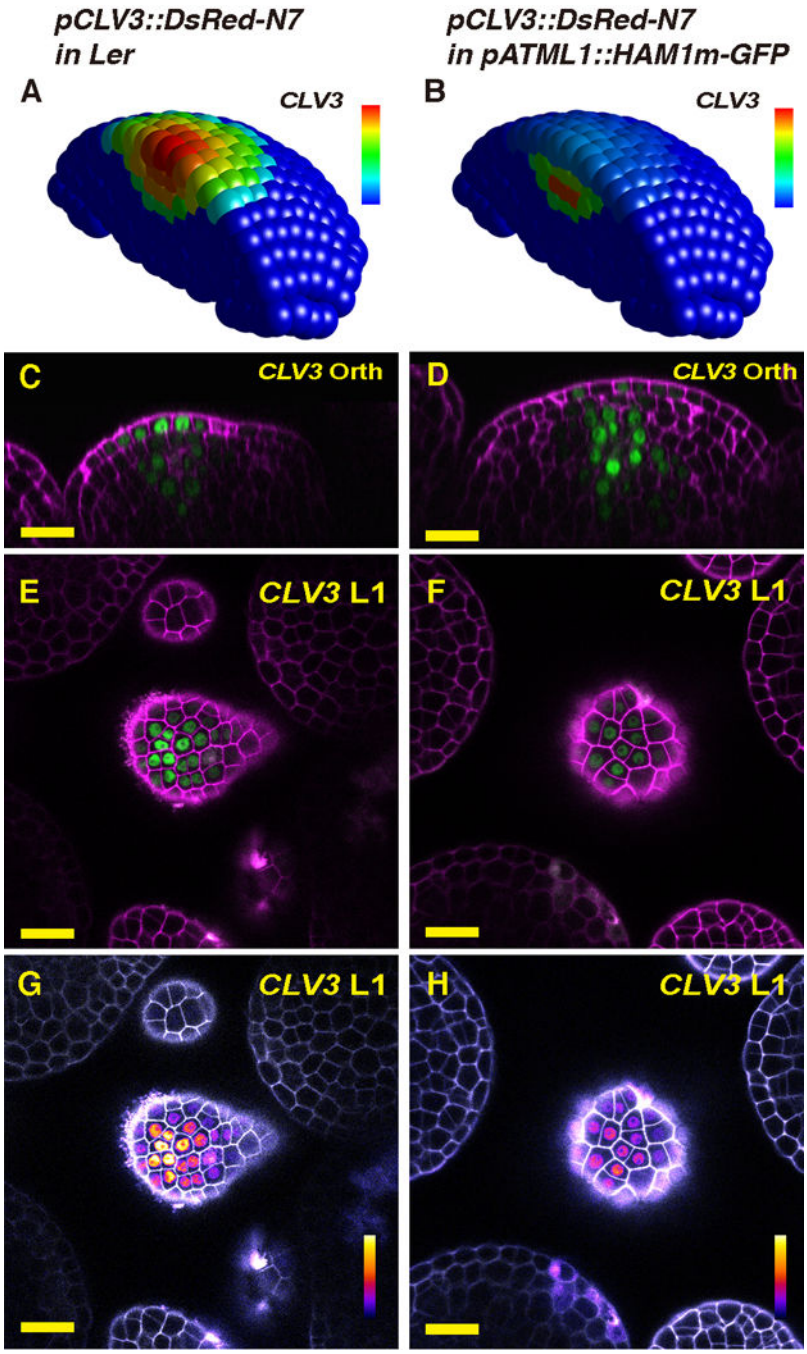

Fig. 2.

Results of HAM expression changes in the L1. (A-B) The simulated *CLV3* expression domain in 3D in both wild type (A) and the *pATML1::HAM1m-GFP* transgenic plant (B) in which *HAM1* is over-expressed in the epidermis. The *CLV3* mRNA levels are indicated by color, with a gradient from red (maximum, 0.86 arbitrary units, a.u.) to blue (0). (C-H) Validation of the computational simulation through confocal live-imaging of a *pCLV3::DsRed-N7* (green) reporter in a *pATML1::HAM1m-GFP* transgenic plant. Orthogonal (C-D) and transverse section (E-H) views of the same wild type (L*er*) plant (C,

E, G) or the same *L1-HAM* transgenic plant (D, F, H) are shown. PI counterstain is represented in purple (C-F) or gray (G-H), and the relative *pCLV3::DsRed-N7* signal intensity is indicated by color (G-H). Scale bar: 20 μm; color bar (G-H): fire quantification of signal intensity. Here and elsewhere in this report, the whole SAM template was used for all of the simulations, but only a half of the SAM is represented, for visualization of cells in inner layers.

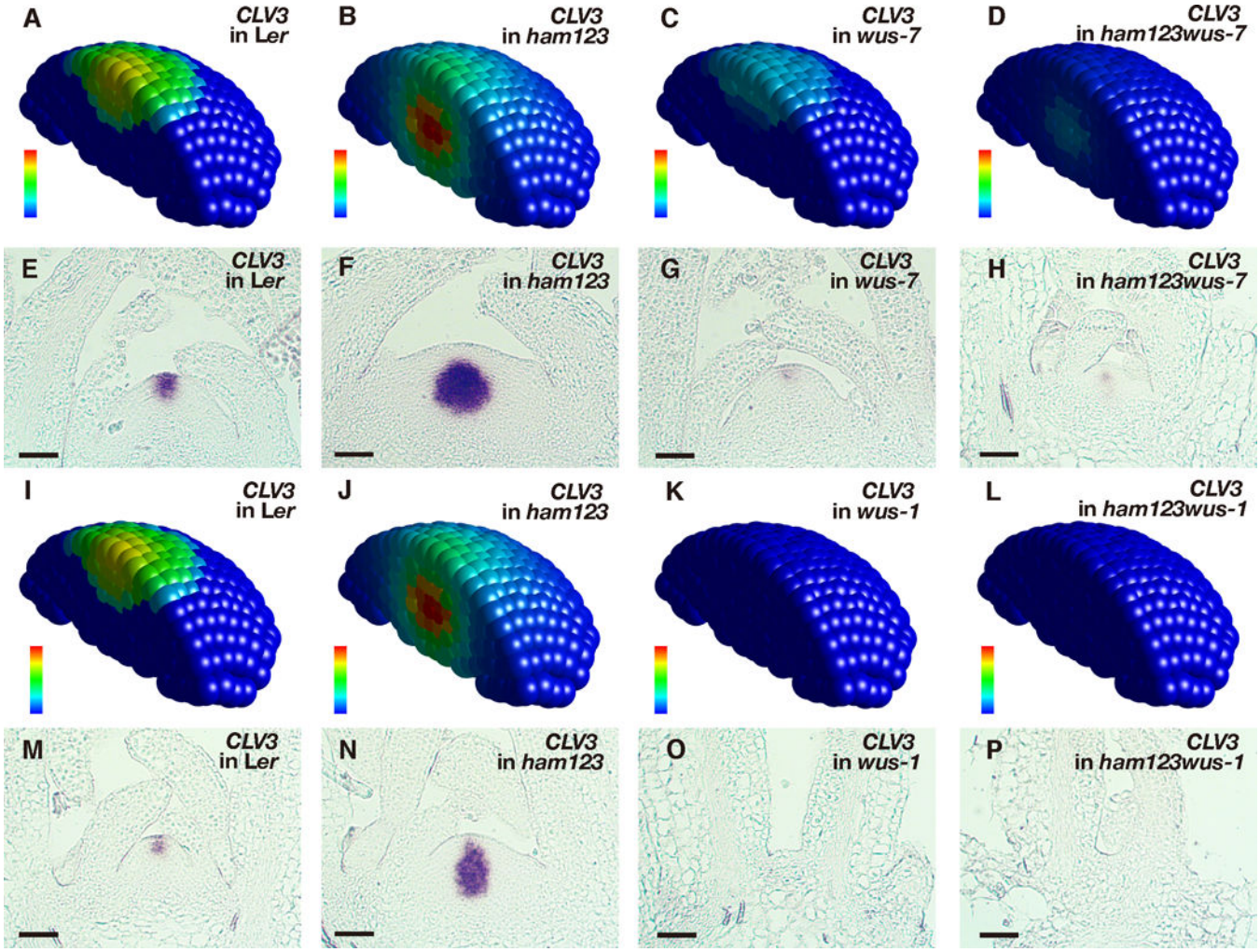

Fig. 3.

Model prediction and experimental validation in SAMs of different genotypes. (A-D) Simulated *CLV3* mRNA levels in 3D in different genotypes including wild type (A), *ham1;2;3* (B), *wus-7* (C), and *wus-7;ham1;2;3* (D). (E-H) Validation of the computational simulation through *in situ* hybridization to *CLV3* RNA in the SAMs of wild type (L*er*) (E), *ham1;2;3* (F), *wus-7* (G), and *wus-7;ham1;2;3* (H) at the same developmental stage (30 days after germination, DAG) in the same experimental conditions. (I-L) Simulated *CLV3* mRNA levels in 3D in different genotypes including wild type (I), *ham1;2;3* (J), *wus-1* (K), and *wus-1;ham1;2;3* (L). (M-P) Validation of the computational simulation through RNA *in situ* hybridization of *CLV3* in the SAMs of wild type (L*er*) (M), *ham1;2;3* (N), *wus-1* (O), and *wus-1;ham1;2;3* (P) at the same developmental stage (22 DAG) in the same experimental conditions. Simulated *CLV3* mRNA level (A-D, I-L) in each individual cell is indicated by color, with the gradient from red (maximum, 1.15 a.u) to blue (none), and the simulations in (I) and (J) are the same as in (A) and (B), respectively. Scale bar (E-H, M-P): 50 μm.

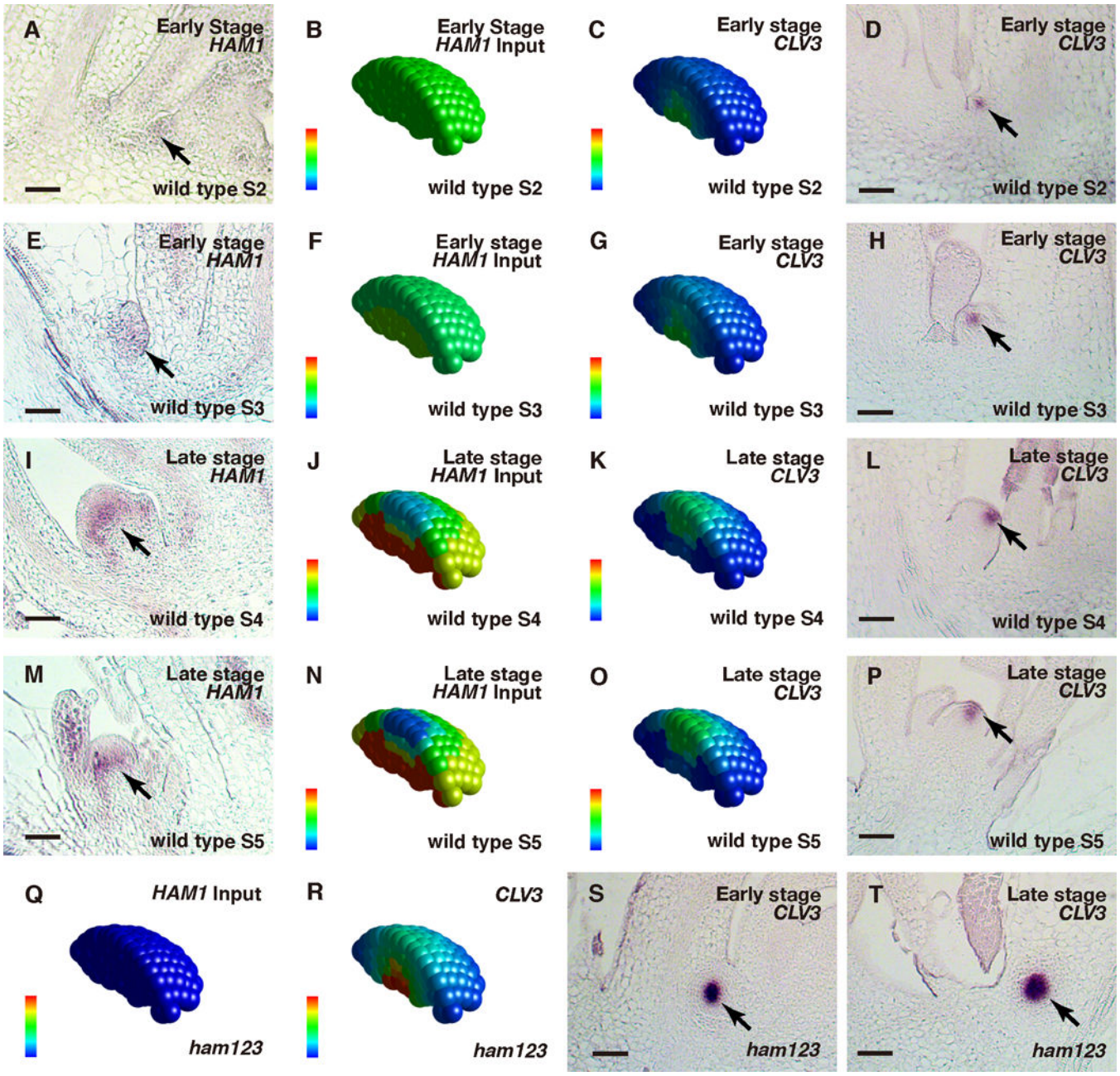

Fig. 4.

Patterning during the *de novo* formation of axillary stem cell niches in wild type (A-P) and in *ham1;2;3* (Q-T). (A, E, I, M) *In situ* hybridization to *HAM1* RNA in wild type, at early (A, E) and late (I, M) stages of axillary meristem (AM) initiation. (B, F, J, N) Levels of HAM concentration in wild-type at early (B, F) and late stages (J, N) as input. (C, G, K, O) Simulated *CLV3* mRNA levels at early (C, G) and late stages (K, O) in wild type. (D, H, L, P) Validation of the simulation through the *in situ* hybridization to *CLV3* mRNA in a wild type AM at early (D, H) and late stages (L, P). (Q) HAM concentration was set at zero in *ham1;2;3* at all stages as the input. (R) Simulated *CLV3* mRNA levels at different developmental stages in *ham1;2;3.* (S-T) Validation of the simulation through RNA *in situ*

hybridization of *ham1;2;3* AMs. The initiation of AMs in *ham1;2;3* was disturbed, and did not follow the well-characterized developmental stages *(23–24)*. The early (S) and late (T) stages of AM initiation in *ham1;2;3* were defined based on the distance of leaf axils from the same main SAM in longitudinal sections. In each individual cell, the relative HAM protein level (input) is indicated by color (blue: 0, red: maximal level 1), and the relative *CLV3* mRNA level (output) is also indicated by color (blue: 0, red: 1.23 a.u). Arrows: *HAM1*-expressing cells (A, E, I, M) and *CLV3*-expressing cells (D, H, L, P, S-T) during new meristem initiation. Scale bar: 50 μm.